Available online at www.sciencedirect.com
SCIENCE DIRECT®
Journal of Nuclear Materials 319 (2003) 108–117
journal of nuclear materials
www.elsevier.com/locate/jnucmat

Post irradiation examination of irradiated americium oxide and uranium dioxide in magnesium aluminate spinel

F.C. Klaassen [a,*], K. Bakker [a], R.P.C. Schram [a], R. Klein Meulekamp [a], R. Conrad [b], J. Somers [c], R.J.M. Konings [c]

[a] Nuclear Research and Consultancy Group (NRG), P.O. Box 25, 1755 ZG Petten, The Netherlands
[b] European Commission, Joint Research Centre, Institute for Energy, P.O. Box 2, 1755 ZG, Petten, The Netherlands
[c] European Commission, Joint Research Centre, Institute for Transuranium Elements, Postfach 2340, 76125 Karlsruhe, Germany

Abstract

To study $MgAl_2O_4$ spinel as inert matrix material for the transmutation of minor actinides, two capsules were irradiated at the high flux reactor in Petten, containing 12.5 wt% micro-dispersed $^{241}AmO_x$ in spinel and 25 wt% micro-dispersed enriched UO_2 in spinel. During irradiation, the initially present ^{241}Am was converted for 99.8% to fission products (50%), plutonium (30%), curium (16%) and ^{243}Am (4%). The UO_2 spinel target experienced a burn-up of 32% fission per initial metal atom. The post irradiation examination of the AmO_x inert matrix target showed swelling of 27 vol.%, and a gas release of 48% for He and 16% for Xe and Kr. The UO_2 inert matrix target also showed a large volumetric swelling of 11%, directed mainly radially. Ceramography on the UO_2 inert matrix target revealed a complete restructuring of the spinel grains upon irradiation and the absence of porosity, suggesting that amorphisation is the main cause of the swelling.

PACS: 61.80.−x; 81.05.Mh; 61.80.Hg; 61.16.−d

1. Introduction

In order to reduce the environmental impact of radioactive waste, innovative concepts are developed to transmute actinides, which make up most of the radiotoxicity of spent fuel. One of the concepts under investigation is the use of inert matrix fuels, which consist of a fissile phase, containing plutonium or americium, embedded in an inert, i.e. transparent to neutrons, matrix phase. The latter can be either a metal, such as zirconium or molybdenum (cermet) or a ceramic material, such as yttria-stabilised zirconia or magnesium alumminate spinel (cercer). Spinel is a prime candidate due to its low neutron absorption cross section, relatively high thermal conductivity (slightly higher than that of UO_2), high melting point and a good compatibility with cladding material and reactor coolant. Moreover, irradiation experiments have shown, that spinel is very stable against neutron irradiation damage [1,2].

The Experimental Feasibility of Targets for TRAnsmutation (EFTTRA) programme [3,4] is a European collaboration programme, set up to study the transmutation of americium and long-lived fission products. Within the EFTTRA programme an extensive study was made of spinel as inert matrix material for Am transmutation [4,5]. The studies, amongst others, focused on the mechanical and chemical stability under neutron irradiation and fission. At the high flux reactor (HFR), a series of irradiation tests have been performed to specifically investigate the irradiation damage by (i) neutrons (EFTTRA T2 [1], T2bis [2]), (ii) neutrons + fission products (EFTTRA T3 [6,7]) and (iii) neutrons + fission products and enhanced helium generation (EFTTRA T4 [8]).

In August 1997 the EFTTRA T4bis/ter irradiation was started in the HFR. Two capsules were irradiated:

* Corresponding author. Tel.: +31-224 564131; fax: +31-224 568608.
E-mail address: klaassen@nrg-nl.com (F.C. Klaassen).

0022-3115/03/$ - see front matter © 2003 Elsevier Science B.V. All rights reserved.
doi:10.1016/S0022-3115(03)00141-7

the T4bis-capsule, containing 12.5 wt% $^{241}AmO_x$ in $MgAl_2O_4$ spinel, and the T4ter-capsule, containing 25 wt% UO_2 (20% enriched in ^{235}U) in spinel. The fissile inclusions in both targets were micro-dispersed, i.e. with diameter ~1 μm. Both targets were irradiated for 26 HFR cycles (a total of 652.55 full power days) to a fast fluence ($E > 0.1$ MeV) neturon influence of 2.13×10^{26} m^{-2} (T4bis) and 1.18×10^{26} m^{-2} (T4ter).

This paper describes the post irradiation examination (PIE) of the EFTTRA T4bis and T4ter samples. Both the T4bis and T4ter capsules were examined non-destructively; the fission gas composition of the capsules and the swelling of the targets were investigated. Destructive PIE, by means of ceramography and electron probe micro-analysis (EPMA), was performed on the UO_2 target (T4ter) only.

2. Target fabrication

2.1. EFTTRA T4bis pellets

The AmO_x inert matrix (T4bis) pellets were fabricated at JRC-ITU, Karlsruhe, in the same batch as the targets for the EFTTRA T4 irradiation [8], and show similar characteristics. The fuel pellets were prepared by an infiltration procedure INRAM [9], which is based on the infiltration of aqueous metal-containing solutions into porous pellets. The green pellets were fabricated by cold-pressing a commercial $MgAl_2O_4$ powder (Baikalox S33CR, Baikowski Chemie) and heat treatment at 925 K. The green pellets, with a density of about 50% TD, were immersed slowly in a nitric acid solution of americium. After removal from the solution, the infiltrated $Am(NO_3)_3$ was converted to AmO_x by thermal treatment at 973 K in an Ar/H_2 atmosphere for 4 h. After sintering for 6 hours under the same atmosphere at 1873 K, the fuel pellets had a density of 96–97% TD.

The pellets contain only the isotope ^{241}Am. The ^{241}Am-content in the pellets is 11.2 ± 0.3 wt% and particle size of the Am-inclusions is typically 2–3 μm. The distribution of Am is not uniform over the pellet. α-Autoradiography and X-ray radiography revealed a cylindrical shell of about 200 μm thickness inside the pellet, with a higher Am-content (about 14 wt%). In regions outside the shell the amount of Am is 9 wt% on average. The characteristics of the T4bis targets are listed in Table 1.

2.2. EFTTRA T4ter pellets

The UO_2 inert matrix (T4ter) pellets consisted of a $MgAl_2O_4$ (spinel) inert matrix with 25 wt% UO_2 (20% enriched in ^{235}U). The mixture of spinel and uranium oxide was made by NRG Petten by means of co-precipitation. Uranium oxide was dissolved in 2 M nitric acid while heating the solution. After cooling, this solution was mixed with a solution of MgO and $Al(NO_3)_3 \cdot 9H_2O$ dissolved in nitric acid. By adding this solution drop-wise to a solution of 6 M NH_4OH a precipitate is formed. The final pH in the solution is 9–10. Neutron activity analysis showed no detectable amount of U, Mg or Al in the remaining solvent (detection limits 0.01, 10, and 0.1 ppm, respectively), indicating that the targets have the intended composition. To remove contaminants and to improve sinteractivity, the precipitate was washed subsequently with water, acetone, toluene, diethylphtalate and again with acetone. The powder was dried at 400 K and calcined at 973 K in air. At this stage the material consists of a mixture of $MgAl_2O_4$ and U_3O_8.

The pellets were pressed by uni-axial pressing. The pellets were sintered at 1873 K in an Ar/H_2 atmosphere for

Table 1
Characteristics of the EFTTRA T4bis and T4ter pellets

	EFTTRA T4bis	EFTTRA T4ter		
		Full pellets	Annular pellets	T4ter capsule total
Number of pellets	10	9	8	17
Pellet mass/g	6.16	3.6	2.3	5.9
Outside diameter/mm	5.39	5.376	5.436	–
Inside diameter/mm	–	–	1.77	–
Height/mm	70.6	40.3	29.2	69.5
Volume/cm^3	1.61	0.91	0.61	1.52
Density/g cm^{-3}	3.82	3.94	3.81	3.88
Density/%TD	96.5	92	89	90.7
$^{241}AmO_x$ content/wt%	12.5	–	–	–
UO_2 content/wt%	–	25	25	25
UO_2 content/vol.%	–	10.47	10.47	10.47
^{235}U enrichment/%	–	20.02	20.02	20.02
$MgAl_2O_4$ content/wt%	87.5	75	75	75

5 h. During sintering the U_3O_8 was converted to UO_2. The characteristics of the pellets that were loaded into the T4ter capsule are given in Table 1. The T4ter capsule was equipped with a thermocouple, measuring the fuel central temperature. Therefore both full pellets and annular pellets were fabricated. To obtain annular pellets, a steel bar with diameter $d = 2.4$ mm was placed in the die during pressing. During sintering, the central hole of the annular pellets reduced in size to $d = 1.77$ mm.

3. Irradiation history

The EFTTRA T4bis/ter irradiation was performed in a central core position of the HFR for a period of 26 HFR cycles, equivalent to 652.55 full power days.

The neutron fluence was monitored by means of eight neutron fluence detectors and four gamma scan wires, symmetrically placed around the T4bis and T4ter fuel stack. The T4bis fuel stack received a uniform flux. The T4ter fissile stack was placed at the top of the sample holder and received a lower flux with a stronger axial variation, due to the neutron flux buckling. The axial variation of the thermal and fast flux, as measured by the gamma scan wires, is depicted in Fig. 1. In Table 2 the fluence values are presented for the centre of the fissile stack of the T4bis and T4ter targets. They are divided into four energy groups, and a separate fast fluence group with $E > 0.1$ MeV. The average total fluence for all energies is 5.18×10^{26} m^{-2} for the T4bis sample and 2.76×10^{26} m^{-2} for the T4ter sample.

Based on the analysis of the fluence monitors, the power profile and the burn-up were computed by MCNP. The generated power in the T4bis capsule was between 40 and 70 W cm^{-1} during the whole irradiation, except for the first few days. The volumetric burn-up of the T4bis target corresponds to 154 GW d m^{-3}. At the end of the irradiation the initial ^{241}Am is completely (to 99.8%) transmuted into fission products (50%), plutonium (30%), curium (16%) and ^{243}Am (4%). It is for the first time that americium has been transmuted to such a high extent with the use of inert matrix concepts.

The generated power in the T4ter capsule decreased from 160 to 40 W cm^{-1} during irradiation. The burn-up of the T4ter target was 32% fissions per initial metal atom (FIMA), corresponding to 217 GW d m^{-3}.

The temperature of the sample-holder during irradiation was monitored by means of 23 thermocouples, positioned at various axial and radial positions near the cladding of the T4bis and T4ter capsules. One central thermocouple was put inside the fuel stack of the EFTTRA T4ter capsule, through the annular pellets. The T4ter central thermocouple had a temperature of 1235 K at the beginning of irradiation. During irradiation the central temperature gradually decreased with the burn-up of ^{235}U, to $T = 675$ K at the end of irradiation. The cladding temperature was kept at a temperature $T \sim 575$ K throughout the whole irradiation. A thorough thermal analysis of the EFTTRA T4bis/ter experiment is beyond the scope of this paper, and will be presented in a subsequent paper, in combination with detailed MCNP computations [10].

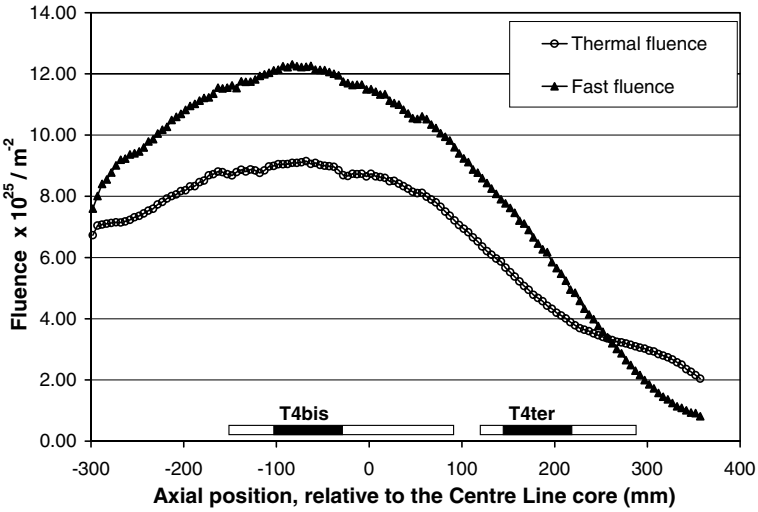

Fig. 1. Axial variation of the fluence in the EFTTRA T4bis and T4ter experiment, as measured by the gamma scan wires. The activation reaction ^{59}Co(n,γ) ^{60}Co was used to deduce the thermal fluence, the reaction ^{54}Fe(n,p) ^{54}Mn to determine the fast fluence. The position of the T4bis and T4ter capsule and both fissile stacks (black) are indicated.

Table 2
Average neutron fluences (ϕ), measured by the fluence detectors in the middle of the fissile stack of the T4bis and T4ter capsules

Group	Energy range	Fluence ($\times 10^{25}$ m^{-2})	
		T4bis	T4ter
ϕ_{IV} (thermal)	$E < 0.683$ eV	9.72	4.59
ϕ_{III}	0.683 eV $< E <$ 64.4 keV	19.78	10.63
ϕ_{II}	64.4 keV $< E <$ 1.353 MeV	14.30	7.92
ϕ_{I}	1.353 MeV $< E <$ 14.92 MeV	8.02	4.45
Fast	$E > 0.1$ MeV	21.28	11.78
Total fluence		51.80	27.58

4. Non-destructive post-irradiation examination

4.1. Profilometry

The size of the outer cladding diameter after irradiation was determined by means of profilometry. In Figs. 2 and 3 the radial swelling of the cladding of the T4bis and T4ter capsules is depicted, together with an X-ray image of the capsule after irradiation.

4.1.1. EFTTRA T4bis capsule

The T4bis outer cladding showed a very distinct profile of peaks, comparable to the profilometry results of the EFTTRA T4 experiment [8]. The swelling profile can be attributed directly to the AmO_x concentration in the fuel pellets. As explained in Section 2.1, there is a cylindrical shell with an increased ^{241}Am-concentration in each T4bis pellet. The Am-rich region is characterised by a locally higher volumetric burn-up and, consequently, a larger swelling. The maxima in the profile of the cladding coincide exactly with the edge of the Am-rich shell, which can be distinguished clearly in the X-ray image in Fig. 2. The minima in the profile correspond to the pellet edge and the middle of the pellet.

The average cladding tube diameter is $D = 6.78 \pm 0.06$ mm. With an initial thickness $d = 0.45$ mm of the cladding tube, the average pellet diameter from the profilometry measurement $D_{pellet} = 5.88 \pm 0.06$ mm, compared to $D_{pellet} = 5.39$ mm before irradiation. The most important conclusion is, that the radial swelling of the T4bis Am inert matrix target is appreciable (~9%), and sensitively depends on the concentration of ^{241}Am in the matrix material. Similar observations were made in the EFTTRA T4 irradiation [8], which contained similar AmO_x targets in spinel, that were irradiated in the HFR to a lower burn-up (shorter irradiation time, cf. Table 4). The axial swelling of the T4bis fuel stack is somewhat smaller (~6.7%) than the radial swelling.

4.1.2. EFTTRA T4ter capsule

The swelling of the T4ter capsule has two regions: a maximum at $z = 38$ mm, and a smaller bump over the full fissile stack length (see Fig. 3). This specific profile can be explained by two main features. The axial neutron flux buckling at the position of the T4ter target caused a larger burn-up at the bottom of the fuel stack. Secondly the swelling at the top was smaller, as the annular pellets contain less material and therefore exhibit less swelling in absolute sense. Moreover there is internal swelling, as the thermocouple is somewhat smaller in diameter than the annular hole in the pellets. The X-ray image, taken after irradiation, indeed shows that all space between the annular pellets and the thermocouple tube was completely filled. The average cladding tube diameter $D = 6.60 \pm 0.02$ mm, which gives, after correcting for the cladding tube thickness, an average pellet diameter $D_{pellet} = 5.70 \pm 0.02$ mm. Note, that the axial swelling of the T4ter target is much smaller (~0.6%) than the radial swelling (~5.2%). In Table 3 the swelling data are summarised, divided in an axial swelling and a radial swelling. The average volumetric swelling is about 27% for the T4bis fuel stack and 11% for the T4ter fuel stack. This is in agreement with other in-pile irradiation tests of spinel inert matrix targets (cf. Section 6).

4.2. Puncturing and gas analysis

In the T4bis target large amounts of He gas were produced due to the decay of the activation product ^{242}Cm ($t_{1/2} = 163$ d) to ^{238}Pu. The absolute pressure in the T4bis capsule, measured by the gas puncturing was 1.74 MPa, consisting mainly (93 vol.%) of He. In Table 4 the computed (by means of MCNP and FISPACT) and measured gas compositions are compared, together with data from the EFTTRA T4 experiment (see [8]). A gas release was found of 48% for He and 16% for Xe and Kr. This is larger than in the EFTTRA T4 irradiation (19.5% He gas release, 5% Xe+Kr gas release), where a high retention of He in the matrix material was observed, accompanied by a large swelling. The He-release is higher than the fission gas release, due to the larger mobility of the (smaller) helium atoms. Note, that the fission gas release is dominated by Xe, which makes up 96% of the fission gas production.

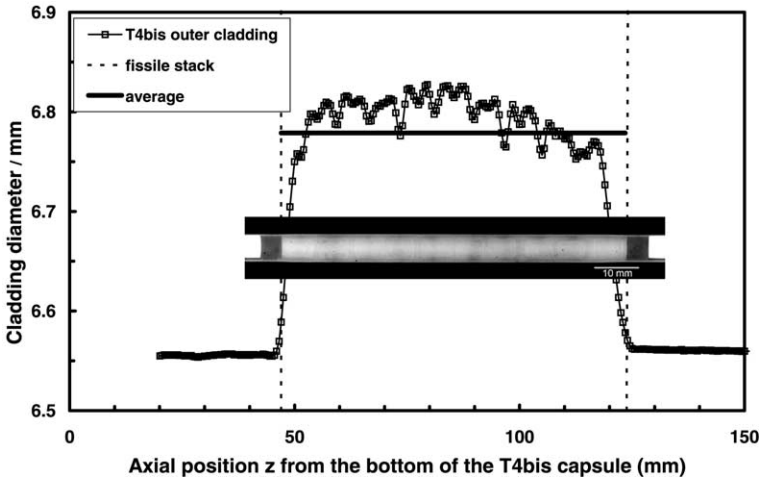

Fig. 2. Outer cladding diameter, as determined by profilometry, and post irradiation X-ray image of the T4bis capsule. The edges of the fissile stack are depicted by the dashed lines. The peaks in the cladding profile correspond to the Am-rich region in the pellet, which are clearly visible in the X-ray image.

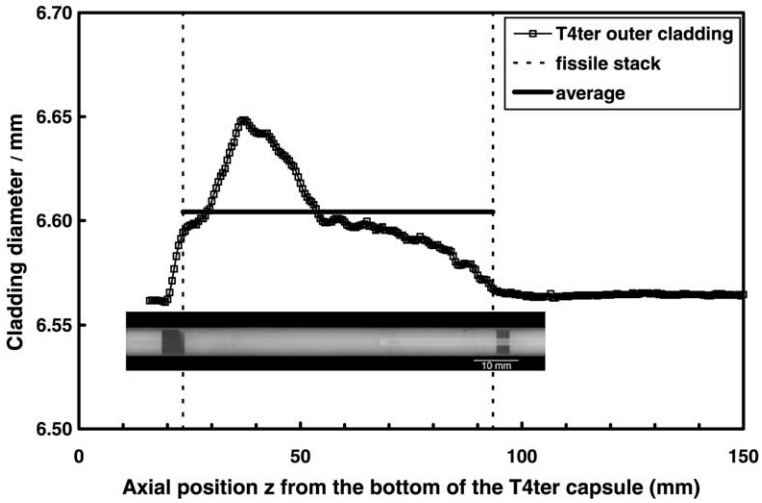

Fig. 3. Outer cladding diameter, as determined by profilometry, and post irradiation X-ray image of the T4ter capsule. The edges of the fissile stack are depicted by the dashed lines. The gap around the thermocouple tube is completely filled due to the swelling of the spinel pellets.

Table 3
Average volumetric swelling of the T4bis and T4ter capsules

Capsule	Pellet diameter/mm	Fissile stack length/mm	Volumetric swelling/vol.%
T4bis, before	5.39	72.51	
T4bis, after	5.88	77.35	
Swelling/%	9.1	6.68	27.0
T4ter, before	5.42	69.46	
T4ter, after	5.70	69.88	
Swelling/%	5.2	0.61	11.1

Note that the data are obtained by combining various measurement techniques, and may differ from the data listed in Table 1.

Table 4
Comparison of the fractional gas release and the burn-up and swelling of the EFTTRA T4 and EFTTRA T4bis irradiations

Irradiation	EFTTRA T4			EFTTRA T4bis		
Irradiation time	358.4 full power days			652.6 full power days		
Depletion[a]	28%			~50%		
^{241}Am burn-up	96%			99.8%		
Swelling	18 vol.% (max., 17 vol.% average)			27 vol.% (average)		
Gas contents	Produced amount (mol)	Released amount (mol)	Fractional release (%)	Produced amount (mol)	Released amount (mol)	Fractional release (%)
He	1.37×10^{-3}	2.66×10^{-4}	19.5	1.84×10^{-3}	8.88×10^{-4}	48
Xe + Kr	2.29×10^{-4}	1.19×10^{-5}	5.2	4.21×10^{-4}	6.85×10^{-5}	16
Total	1.60×10^{-3}	2.78×10^{-4}	17.4	2.27×10^{-3}	9.56×10^{-4}	42

The T4-data are taken from Ref. [8].
[a] The depletion is defined as (number of actinide atoms (BOI) – number of actinide atoms (EOI))/(number of actinide atoms (BOI)) × 100%; BOI: beginning of irradiation and EOI: end of irradiation.

There is an intricate relation between the burn-up, the volumetric swelling, and the gas release. As the temperatures of both irradiations were comparable, the higher burn-up apparently resulted in a high fractional gas release *and* the large swelling of the T4bis capsule. A possible explanation is that at the beginning of the irradiation the helium gas was mostly retained in the matrix, causing a large swelling due to the formation of gas bubbles. At larger burn-up open porosity may have been created, enabling the helium and the other fission gases to be released into the plenum in large amounts. This scenario should be confirmed by the destructive PIE on the T4bis targets, which is planned to take place in the near future.

The gas analysis of the T4ter capsule revealed that a leak occurred in the capsule after irradiation, and air had come into the capsule. The gas puncturing of the T4ter capsule therefore yielded unusable results.

5. Destructive examination of the T4ter target

5.1. Ceramography

In Fig. 4 optical images are shown of an unirradiated (Fig. 4(a)) and irradiated (Fig. 4(b)) T4ter pellet. The latter image was obtained after cutting and subsequent grinding and polishing the T4ter target at the position of maximum swelling. The unirradiated pellet consists of a random mixture of grains of variable size. In the irradiated pellet two remarkable features were observed, namely a disappearance of the grain structure and the absence of porosity. A second cut at a different axial position confirmed that these features are representative for the whole T4ter target. In addition an almost perfectly regular circular crack of radius $r = 2.4$ mm was observed. The swelling of the pellet has completely closed the gap between the fuel and the cladding. In the middle of the

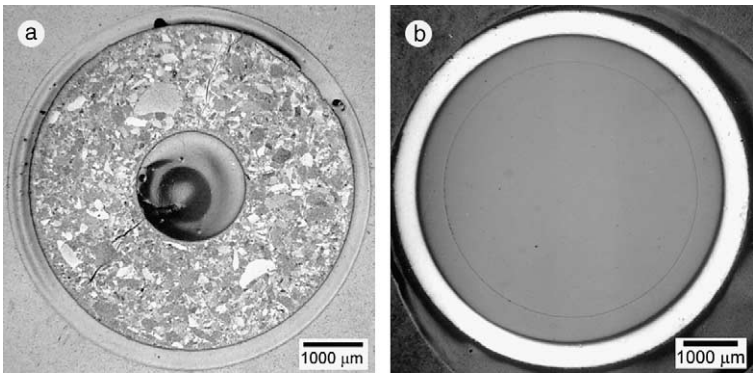

Fig. 4. Ceramographic images of (a) unirradiated (annular) T4ter pellet, and (b) irradiated (full) pellet. The original grain structure of the unirradiated pellet has completely disappeared and the swelling has completely closed the gap between pellet and cladding (white).

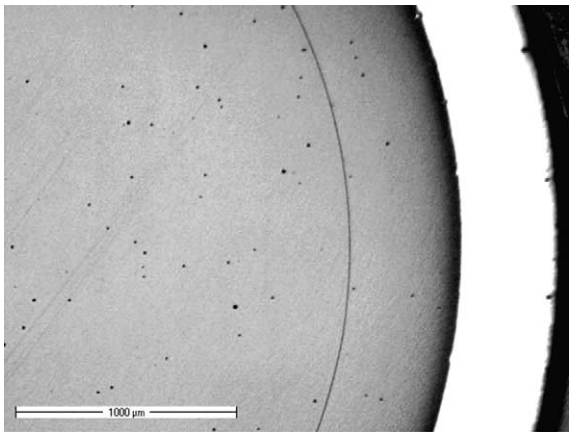

Fig. 5. Ceramographic image (detail) of the full EFTTRA T4ter pellet (Fig. 4(b)) after irradiation. A remarkably small porosity is found in the irradiated pellet, and almost no crack structure.

target also small radial cracks were found, although with the ceramograph they were almost invisible. Probably crack-healing has taken place during irradiation.

In Fig. 5 a detail is shown of the irradiated pellet from Fig. 4(b). There is a porosity of 0.52%, the circular crack included. This is unexpectedly low in view of the large burn-up and swelling. A possible explanation for the low porosity could be that the samples contain many very small pores, which cannot be seen due to the resolution of the optical microscope, which is typically ~5 μm. Therefore the measured porosity could be an underestimation of the actual porosity.

5.2. Electron probe micro-analysis

By means of EPMA, the distribution of the UO_2 and spinel phases in the irradiated fuel has been investigated in detail. For this purpose X-ray absorption images, element mappings and point/line scans were made at various positions on the target of Fig. 4(b).

In Fig. 6, two absorption images are depicted, taken in the middle (a) and near the edge (b) of the irradiated T4ter pellet. In the pellet centre the sample is homogeneous, apart from some radial cracks (white). These cracks were observed by ceramography as well, but hardly visible due to crack healing. In addition a larger white spot was found (lower right corner of Fig. 6(a)), which is either a pore or MgO. Near to the edge of the sample a more inhomogeneous distribution was observed, as is shown in Fig. 6(b). Note, that in Fig. 6(b) the dark line running through the middle is no crack, but belongs to a uranium phase. The differences observed between the centre and the edge of the sample are temperature induced. As the temperature in the middle of the pellet is higher, a different restructuring of the UO_2 and spinel has taken place in the pellet centre than at the edge.

The EPMA element maps (Fig. 7) show the effect of the irradiation on the distribution of various elements. The distribution of aluminium, oxygen and the fission products was homogeneous. However, the distribution of uranium and magnesium was complementary, i.e. where there is a large concentration of U, there is less Mg and vice versa. This is shown in Fig. 7(a)–(d). In Fig. 7(a) and (b) the mappings of U and Mg are shown in the centre of the pellet. In Fig. 7(c) and (d) the mappings of U and Mg are shown, taken at 300 μm from the edge of the sample. The mappings confirm the larger inhomogeneity near the rim of the pellet. In addition, the maps in the centre seem to indicate a lower Mg density in the centre of the target. Although the maps of Fig. 7(b) and (d) were both measured for the same amount of time, the overall number of white pixels clearly differs.

To investigate in more detail the chemical composition and homogeneity of the target, quantitative EPMA

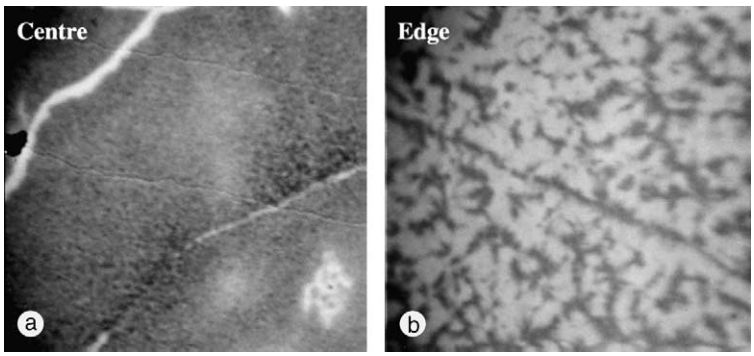

Fig. 6. 70×70 μm^2 EPMA absorption images of the EFTTRA T4ter target after irradiation (a) in the pellet centre, (b) 300 μm from the pellet edge. Whereas the pellet centre has a reasonably homogeneous structure, the matrix near the pellet edge consists of U-rich (dark) and U-poor (bright) phases. The latter contain more Mg than the U-rich regions.

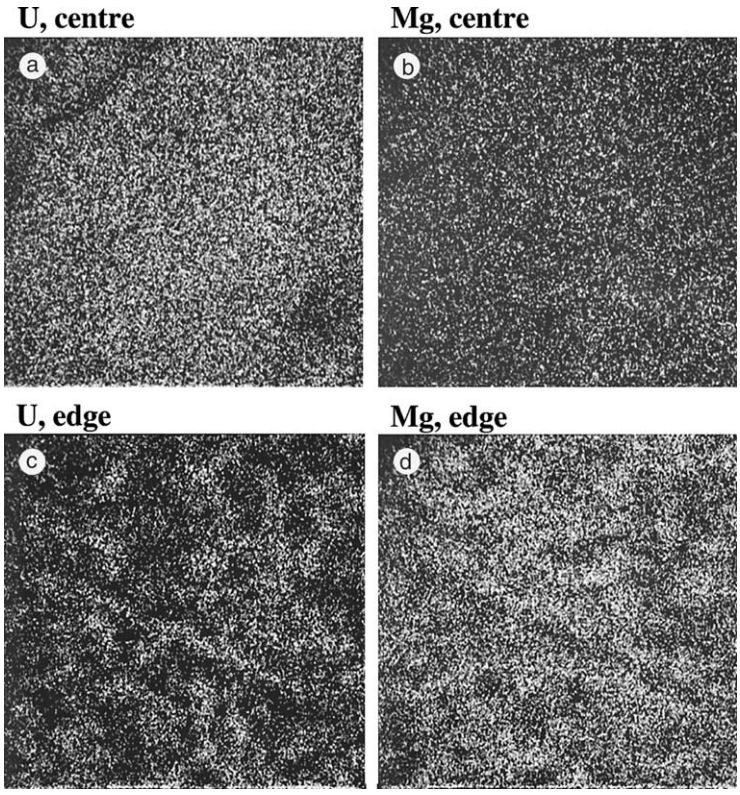

Fig. 7. (a) 70×70 μm^2 EPMA mapping of U in the centre region of the pellet, measured for 7 min. (b) Idem for Mg, measured for 30 min. (c) 70×70 μm^2 EPMA mappings of U, taken 300 μm from the edge of the pellet, measured for 7 min. (d) Idem for Mg, measured for 30 min.

measurements were performed in the centre and at the edge of the pellet. Three point scans were taken in the middle of the sample, where the mappings showed a homogeneous distribution of spinel and UO_2 phases. Secondly a line scan of 48 μm was made at 300 μm from the edge of the sample, going through the bright and dark phases, which were observed in the X-ray absorption picture (Fig. 6(b)). The results of the quantitative EPMA scans are given in Table 5. In the pellet centre and in the U-rich regions near the edge, there is a reduced Mg content compared to Al. It has been reported for ROX-fuels (mixture of spinel and $(Y,Pu/U,Zr)O_{2-x}$ as fissile component), that spinel decomposes during irradiation, with MgO disappearing out of the spinel [11,12]. However this effect was observed at much higher irradiation temperature (1700 K) than the T4ter targets experienced (~1275 K). Possibly the spinel phase decomposed partially into Al_2O_3 and MgO, of which the latter diffused more to the edge of the pellet. A second explanation is, that sub-stoichiometric spinel phases (i.e. Mg-poor $Mg_{1-x}Al_2O_{4-x}$) and separate MgO phases have formed during irradiation. From a line scan near the

Table 5
Average element composition, measured by quantitative EPMA scans in the pellet centre and 300 μm from the pellet edge

Element fraction	Point scans in the pellet centre	Line scan near the edge, U-rich region	Line scan near the edge, U-poor region
U/wt%	17.8 ± 1.7	23.2 ± 5.5	9.7 ± 4.3
U/at.%	2.2 ± 0.3	2.5 ± 0.8	0.9 ± 0.4
Mg/at.%	10.7 ± 0.5	10.1 ± 1.6	11.1 ± 1.0
Al/at.%	28.6 ± 1.1	26.8 ± 3.8	21.1 ± 2.8
$N_{Mg} \cdot N_{Al}^{-1}$/atom/atom	0.37	0.38	0.53

The latter results are listed separately for the U-rich and U-poor regions.

edge of the pellet, we found alternating U-rich and Mg-rich regions. Note that the average U-content over the line scan near the edge is 2.1 at.%, the same as in the centre of the fuel pellet. In the U-rich region at the edge a sub-stoichiometric (Mg-poor) spinel composition is found, with a similar Mg:Al ratio as in the centre of the pellet. In the region with a reduced uranium content, the spinel seems to be stoichiometric, as the ratio between the amount of magnesium and aluminium is 1:2.

6. Discussion

The PIE results of the T4bis target are directly comparable to the EFTTRA T4 irradiation [8], which contained the same amount of $^{241}AmO_x$ in spinel. As the irradiation time of the T4bis experiment is almost twice as long, the swelling and fractional gas release have also increased. From the destructive PIE of the EFTTRA T4 targets, a high porosity was found due to the accumulation of helium in gas bubbles [8]. Although the T4bis targets have not been investigated by ceramography, the helium-induced porosity in the T4bis pellets is likely to be even larger, due to the higher helium production.

The large swelling of the T4ter target is characteristic for micro-dispersed UO_2 particles in spinel, which is subject to uniform fission product damage in the whole matrix. In macro-dispersed UO_2 targets, investigated in the EFTTRA T3 irradiation, less swelling was observed [6]. Yamashita et al. [12] obtained similar swelling results from irradiation tests of homogeneously mixed and particle dispersed ROX fuel targets. The former exhibited a volumetric swelling of 10.2 vol.%, comparable to the swelling of the T4ter target. In an irradiation test of spinel with micro-dispersed UO_2 inclusions, performed in the French SILOE reactor (THERMHET irradiation), strong swelling was also observed (~15 vol.%), even at a much lower burn-up of 1.3% FIMA [13]. X-ray diffraction on this micro-dispersed THERMHET target showed that the spinel had become amorphous [14]. Amorphisation and subsequent swelling of spinel due to high-energy ion bombardment was also found by Wiss et al. [15]. The amorphisation of spinel, induced by fission products, is therefore a plausible explanation of the T4ter swelling behaviour.

A second cause for swelling may be the creation of porosity, which may have been underestimated in the T4ter target due to pores, that are too small to be resolved by ceramography. In this scenario the produced fission gases also contribute significantly to the swelling. The central temperature during irradiation (maximum ~1275 K at the beginning of irradiation) is too low to enable a large mobility of fission gas atoms. Therefore fission gas atoms might form small inclusions, smaller than the resolution of the optical microscope (~5 μm).

Note, that the swelling of the T4bis capsule is much larger than the T4ter capsule, despite a lower volumetric burn-up. This indicates, that in the T4bis target the produced helium significantly contributes to the swelling, whereas in the T4ter target amorphisation seems to be the main contributor to the volume increase.

7. Conclusions

In the EFTTRA T4bis and T4ter irradiation experiment two capsules with $MgAl_2O_4$ (spinel) inert matrix fuel were successfully irradiated at the HFR. The T4bis capsule contained 12.5 wt% AmO_x in spinel, the T4ter capsule 25 wt% UO_2 (20% enriched in ^{235}U) in spinel. During irradiation nearly all ^{241}Am and fissile ^{235}U has been transmuted.

The results of the EFTTRA T4bis and T4ter irradiation illustrate the behaviour of spinel under fission product damage and enhanced helium production. Both the swelling and fission gas release are large. The rearrangement of the spinel into stoichiometric and non-stoichiometric phases, as found in the T4ter target, raises questions concerning the chemical stability of spinel.

On the other hand, to our knowledge, it is for the first time, that the concept of heterogeneous inert matrix targets has been successfully applied to the transmutation of an americium-containing rodlet to such a high actinide depletion (~50%). The large swelling and gas release are disadvantageous, but in the fuel design these can be accommodated, for example by using targets with an initial porosity and larger gas plenum's. Alternatively, other inert matrix targets, such as yttria-stabilised zirconia as a solid solution, eventually in combination with spinel (ROX-fuel), seem to exhibit less swelling [16].

References

[1] R.J.M. Konings, K. Bakker, J.G. Boshoven, R. Conrad, H. Hein, J. Nucl. Mater. 254 (1998) 135.
[2] E.A.C. Neeft, R.J.M. Konings, K. Bakker, J.G. Boshoven, H. Hein, R.P.C. Schram, A. van Veen, R. Conrad, J. Nucl. Mater. 274 (1999) 78.
[3] J.-F. Babelot, R. Conrad, H. Gruppelaar, G. Mühling, M. Salvatores, G. Vambenepe, in: Proceedings Global 1997, Yokohama, 1997, p. 676.
[4] N. Chauvin, R.J.M. Konings, Hj. Matzke, J. Nucl. Mater. 274 (1999) 105.
[5] D. Warin, R. Conrad, D. Haas, G. Heusener, P. Martin, R.J.M. Konings, R.P.C. Schram, G. Vambenepe, in: Proceedings Global 2001, Paris, 2001, available on CD-ROM.
[6] E.A.C. Neeft, K. Bakker, R.P.C. Schram, J. Nucl. Mater., Proceedings of ERMT II.

[7] E.A.C. Neeft, K. Bakker, H.A. Buurveld, J. Minkema, A. Paardekooper, R.P.C. Schram, C. Sciolla, O. Zwaagstra, B. Beemsterboer, J.R.W. Woittiez, P. van Vlaanderen, W.J. Tams, H. Hein, R. Conrad, A. van Veen, Prog. Nucl. Energy 38 (2001) 427.
[8] R.J.M. Konings, R. Conrad, G. Dassel, B.J. Pijlgroms, J. Somers, E. Toscano, J. Nucl. Mater. 282 (2000) 159.
[9] K. Richter, A. Fernandez, J. Somers, J. Nucl. Mater. 249 (1997) 121.
[10] F.C. Klaassen, R. Klein Meulekamp, J. Nucl. Mater., in preparation.
[11] N. Nitani, K. Kuramoto, T. Yamashita, Y. Nakano, H. Akie, in: Proceedings Global 2001, Paris, 2001, available on CD-ROM.
[12] T. Yamashita, K. Kuramoto, H. Akie, Y. Nakano, N. Nitani, T. Nakamura, K. Kusagaya, T. Ohmichi, J. Nucl. Sci. Technol. 39 (2002) 865.
[13] V. Georgenthum, N. Chauvin, J. Noirot, C. Berlanga, D. Brenet, in: Proceedings Global 1999, Jackson Hole, Wyoming, 1999, available on CD-ROM.
[14] J. Noirot, L. Desgranges, N. Chauvin, V. Georgenthum, J. Nucl. Mater. (2003), ERMT.
[15] T. Wiss, Hj. Matzke, V.V. Rondinella, T. Sonoda, W. Assmann, M. Toulemonde, C. Trautmann, Prog. Nucl. Energy 38 (2001) 281.
[16] R.R. van der Laan, R.P.C. Schram, F.C. Klaassen, K. Bakker, T. Yamashita, F. Ingold, these Proceedings. doi:10.1016/S0022-3115(03)00143-0.